

# Study on nonlinear dynamic behavior and stable operation region of single-phase photovoltaic inverter

Peng Li, Pinqun Jiang, Zhixian Liao and Rui Fan

College of Electronic Engineering, Guangxi Normal University, Guilin 541004, China  
zhixianliao@mailbox.gxnu.edu.cn

**Abstract.** In order to design a photovoltaic inverter with excellent performance, the second-order photovoltaic inverter circuit model under current loop proportional control is established in this paper, the discrete iterative model of system is also obtained. The nonlinear behavior of system is analysed in detail through bifurcation diagram, folding diagram and the phase diagram of output current ( $i$ ) and output voltage ( $u_c$ ). The simulation model is constructed in Matlab/Simulink, and the correctness of theoretical analysis is verified through time domain waveform and phase-space map. The influence of bifurcation and chaos on system spectrum is analysed from the frequency domain. According to the Jacobian matrix of system, the stable operation region of system is given. The experiment shows that the correct selection of circuit parameters is important for the stable operation of system.

## 1. Introduction

In recent years, as one of the effective means to solve the energy crisis, photovoltaic power generation has become a hot topic for people to study [1]. The inverter is a core device in photovoltaic system, and it is also a kind of strong nonlinear power equipment. There are nonlinear phenomena such as double period bifurcation, fast-and slow-scale instability, boundary collision bifurcation, and chaos [2-4]. These nonlinear phenomena have a bad effect on the stable and reliable operation of the power equipment, and even lead to sudden collapse of the power system [5-6]. Therefore, the study of these nonlinear dynamic behaviors is conducive to optimizing the circuit design and improving the stability and reliability of system.

Many scholars have already done some researches on the nonlinear phenomenon of inverter. Literature [7] firstly discussed the discrete modeling and nonlinear phenomena of H-bridge inverter and extended the dynamic behavior of power electronic converter into inverter circuit. Literature [8-9] established a discrete model of a sinusoidal pulse width modulation H-bridge inverter, and performed a detailed analysis of its nonlinear behavior and stability. Literature [10] analyzed the bifurcation and chaos phenomena of H-bridge inverter under unipolar sinusoidal pulse width modulation. In the above studies, the discrete modeling and dynamic behavior of typical first-order L-filter-based H-bridge inverter are discussed for the convenience of analysis. However, the second-order LC filter inverter has the advantages of smaller ripple and lower harmonic than the first-order L-filter inverter, and is more practical in practical systems.

Nowadays, the research on nonlinear dynamic behaviour of inverter [11-13] mainly focuses on proportional coefficient  $K$ , while other parameters have little research. Moreover, due to the large fluctuations in the input parameters of photovoltaic system, it will lead to system running in an unstable state [14]. In view of the above issues, this paper aims to study the nonlinear phenomenon of second-order photovoltaic inverter with LC filter under current control. According to the actual



operating environment of system, the voltage  $U_{pv}$  on the DC side of inverter is selected as the bifurcation parameter. The bifurcation diagram, folding diagram, phase trace diagram, and frequency spectrum diagram are used to analyze the evolution of system from stable state to chaotic state. The simulation model of system is established in Matlab/Simulink, the correctness of theoretical analysis is verified. Finally, the stable operating domain of system is determined. The research results have important reference value for the design, operation and maintenance of actual circuit system.

## 2. Discrete model of second-order photovoltaic inverter

### 2.1. Schematic of photovoltaic system

Figure 1 shows a typical second-order LC filter photovoltaic inverter circuit under current loop proportional control.  $U_{pv}$  is DC-side input voltage supplied by the photovoltaic cell with an MPPT function. S1-S4 are the power switching tubes. Inductor  $L$  and capacitor  $C$  act as filter circuit. Load resistance  $R$  is output. Output current  $i$  is compared with reference current  $i_{ref}$  to get error signal  $i_e$ , send  $i_e$  to a proportional regulator to get modulated signal  $i_{con}$ , triangular wave  $i_{tri}$  is compared with  $i_{con}$  to generate SPWM, which drives S1-S4 to track sinusoidal current  $i_{ref}$ .

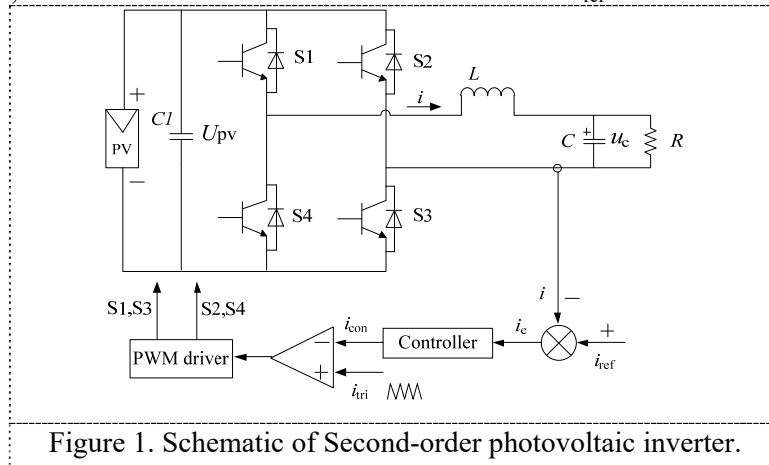


Figure 1. Schematic of Second-order photovoltaic inverter.

### 2.2. Discrete iterative model

The system has two operating states during a switching period  $T$ . State 1: S1 and S3 are on, S2 and S4 are off; State 2: S2 and S4 are on, and S1 and S3 are off. The state equation is as follows.

$$\text{State 1 : } \begin{cases} \frac{di}{dt} = -\frac{1}{L} u_c + \frac{U_{pv}}{L} \\ \frac{du_c}{dt} = \frac{1}{C} i - \frac{1}{RC} u_c \end{cases} \quad (1)$$

$$\text{State 2 : } \begin{cases} \frac{di}{dt} = -\frac{1}{L} u_c - \frac{U_{pv}}{L} \\ \frac{du_c}{dt} = \frac{1}{C} i - \frac{1}{RC} u_c \end{cases} \quad (2)$$

Where,  $i$  and  $u_c$  are state variables, setting  $X = [i, u_c]$ , the system state equation can be expressed as follows.

$$\frac{dX}{dt} = A_i X + B_i, \quad (i = 1, 2.) \quad (3)$$

$$\text{Where, } A_1=A_2=A=\begin{bmatrix} 0 & -\frac{1}{L} \\ \frac{1}{C} & -\frac{1}{RC} \end{bmatrix}, B_1=\begin{bmatrix} \frac{U_{pv}}{L} \\ 0 \end{bmatrix}, B_2=\begin{bmatrix} -\frac{U_{pv}}{L} \\ 0 \end{bmatrix}.$$

According to the main idea of stroboscopic mapping model method, solve equation (3) to get the main circuit discrete model, which is expressed as follows.

$$X_{n+1} = e^{AT} X_n + e^{A(1-d_n)T} [e^{Ad_n T} - E] A^{-1} B_1 + [e^{A(1-d_n)T} - E] A^{-1} B_2 \quad (4)$$

Where,  $d_n$  is duty ratio during the  $n^{\text{th}}$  switching cycle, its value is determined by control part and can be expressed as follows.

$$d_n = \begin{cases} 0 & (d_n < 0) \\ d + K(i_{refn} - \alpha X_n) & (0 \leq d_n \leq 1) \\ 1 & (d_n > 1) \end{cases} \quad (5)$$

Where,  $d$  is a constant,  $K$  is proportional regulate coefficient,  $\alpha = [1 \ 0]$ .

### 3. Nonlinear dynamic behavior of system

In the actual operating environment of system, the voltage  $U_{pv}$  on the DC-side of inverter is most susceptible to outside interference after the proportional coefficient  $k$  is determined. This section uses bifurcation diagram and folding diagram to analyze the influence of DC-side voltage  $U_{pv}$  on system performance. Then use Matlab/Simulink platform to build circuit model, and obtain the time domain waveforms and frequency spectrum of system under different voltages ( $U_{pv}$ ) to verify the correctness of theoretical analysis. Basic circuit parameters are set as follows:  $U_{pv}=250\text{V}$ ,  $L=10\text{mH}$ ,  $R=5\Omega$ ,  $C=50\mu\text{F}$ ,  $T=100\mu\text{s}$ ,  $K=0.3$ ,  $d=0.4$ ,  $f=50\text{Hz}$ ,  $i_{ref}=10\sin(2\pi ft)$ .

#### 3.1. Bifurcation diagram

In this section, the bifurcation diagram of photovoltaic voltage  $U_{pv}$ , proportional coefficient  $K$ , and filter inductance  $L$  are show system has a nonlinear behavior. Figure 2 shows that the system changes from a steady state to a chaotic state with the photovoltaic voltage increases from 200V to 600V, and the bifurcation behavior occurs when voltage is 339V. Fixed photovoltaic voltage  $U_{pv}=250\text{V}$ , Figure 3 shows that the system gradually enters a chaotic state with the proportional coefficient increases from 0.2 to 0.8, and if the system runs stably, the maximum adjustment value of  $K$  is 0.4. Figure 4 shows that the system changes from a stable cycle 1 to a chaotic state when the inductance  $L$  decreases, but when the inductance  $L$  decreases further, the system returns from the chaotic state to cycle 2. Therefore, the system should reasonably select circuit parameters to prevent the system from operating in an unstable state.

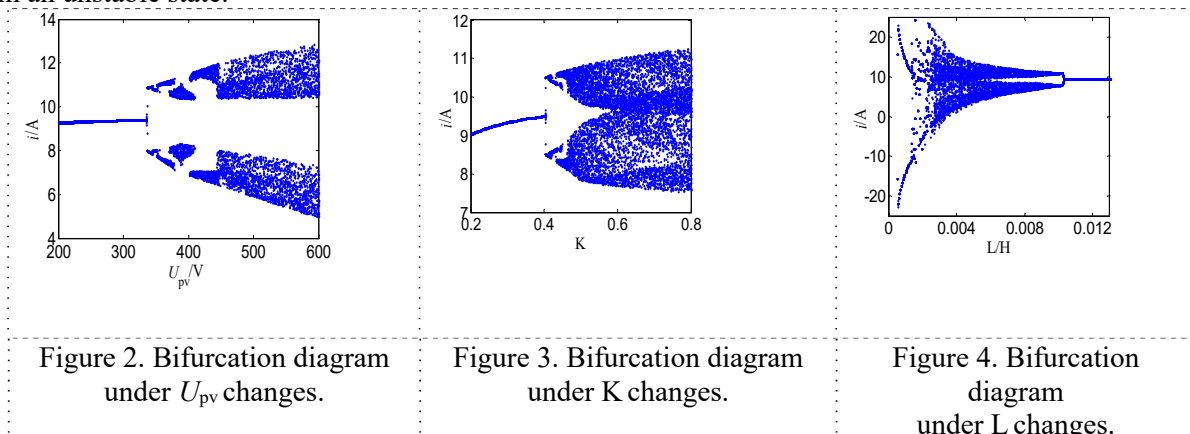


Figure 2. Bifurcation diagram under  $U_{pv}$  changes.

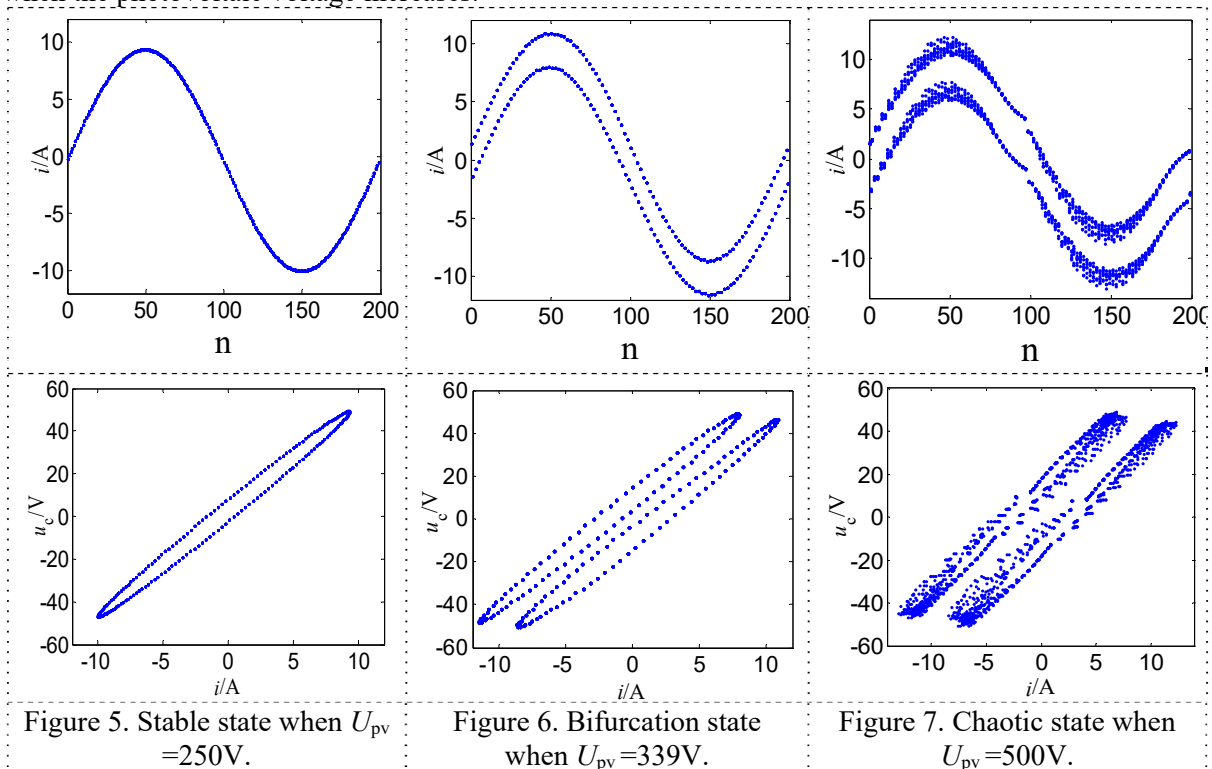
Figure 3. Bifurcation diagram under  $K$  changes.

Figure 4. Bifurcation diagram under  $L$  changes.

### 3.2. Folding diagram

Photovoltaic voltage  $U_{pv}$  is an important parameter that affects system performance. According to Figure 2, this section selects the different bifurcation parameter ( $U_{pv}$ ) values and draws the folding diagram of system. The output current waveform is generally concerned when studying the nonlinear phenomenon of inverter, while the output voltage is ignored. In fact, the phase diagram of output voltage and output current is also a good way to observe the state of system. This method does not require complex computation and can directly reflect the state of system. The phase diagram ( $i-u_c$ ) is given in this section.

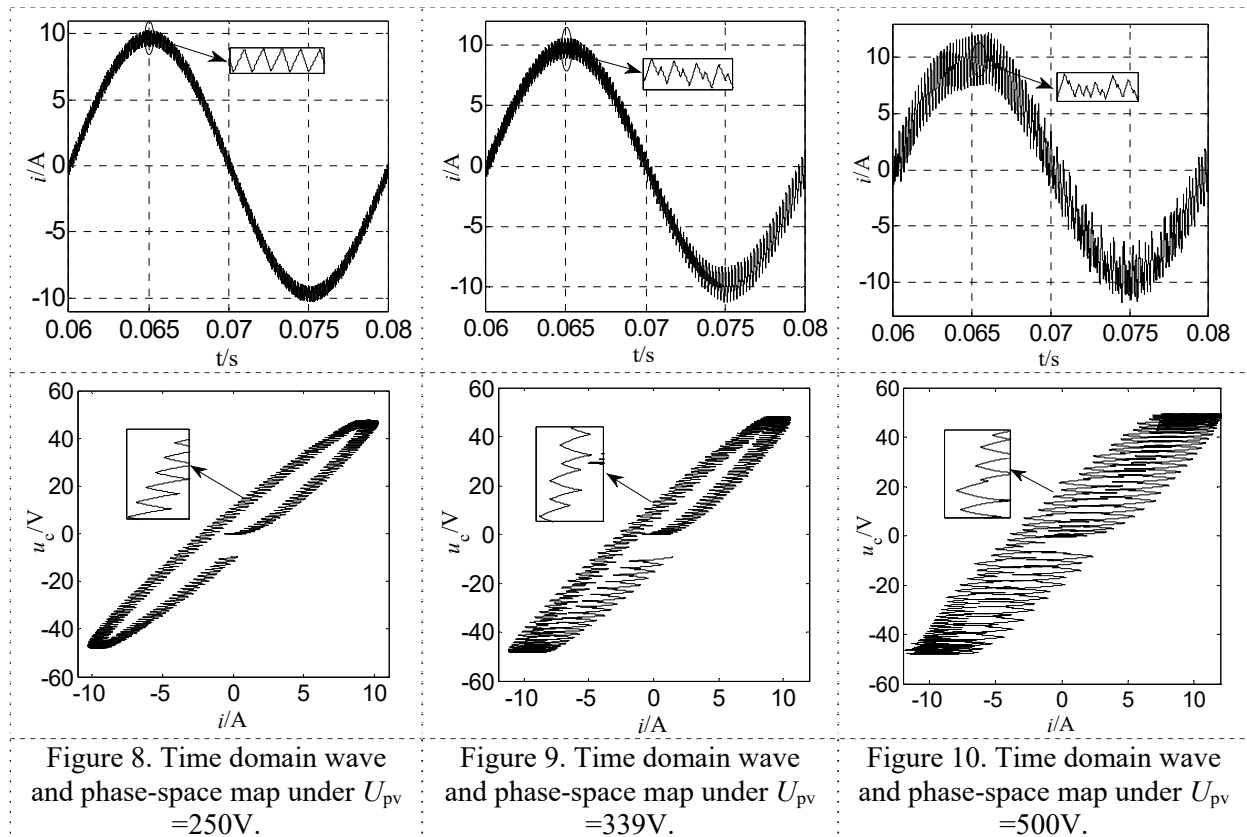
In Figure 5, all the sampling points make up a smooth curve, and phase diagram of  $i-u_c$  is a closed curve, it shows that the system is in steady state; In Figure 6, there are two curves in the folding diagram, two closed curves also appear in the phase diagram, this explains that the system is in bifurcation state; In Figure 7, many cluttered sampling points appear in the diagram, there are also a lot of irregular points in the phase diagram, the system is in a chaotic state at this time. As described above, the simulation results are consistent with Figure 2, and the stability of system will be worse when the photovoltaic voltage increases.



### 3.3. Time domain waveform and phase-space map

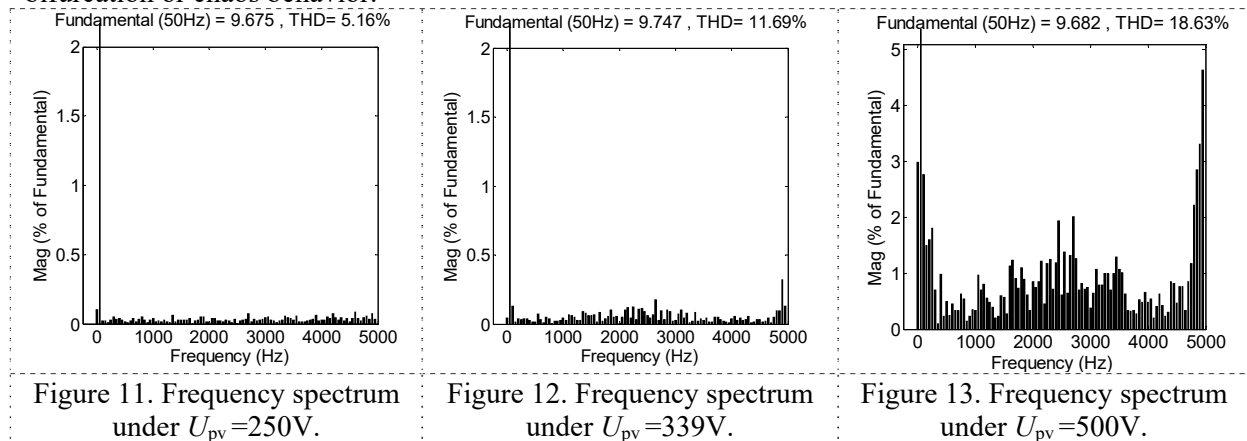
The simulation model of actual circuit is established in Matlab/Simulink platform, and the circuit parameters are consistent with the circuit parameters selected when analyzing the bifurcation diagram. The time domain waveforms and phase-space maps for different photovoltaic voltages are shown in Figure 8, 9, 10.

The state of system can be observed from output current waveform and phase-space map. It can be seen from the local zoom in each group of figures, figure 8 shows that the system is operating in a steady state; figure 9 shows that the system is operating in a bifurcation state; figure 10 shows that the system is operating in a chaotic state. When comparing Figures 8–10, as the voltage increases, the time-domain waveform oscillates more violently and the phase-space map becomes unregulated, that is, the instability of system is more evident. The above result verifies the correctness of theoretical analysis is described in section 3.2.



### 3.4. Frequency spectrum

From the frequency domain perspective, the effects of bifurcation and chaos on the system spectrum are analysed. In figure 11, the system is stable, and there are also few harmonics, THD=5.16%; In figure 12, the system is in a bifurcation state, and the amount of harmonics slightly increased, THD=11.69%; In figure 13, the system is in a chaotic state, and harmonic components increase significantly, THD=18.63%. As described above, the instability of system increases the harmonic content of output current and directly affects the power supply quality of system, but from another perspective, it can judge whether the system has failed through the harmonic content of system. If the harmonic content of system increases suddenly, it can be considered whether the system appeared bifurcation or chaos behavior.



## 4. Stable operation region of system

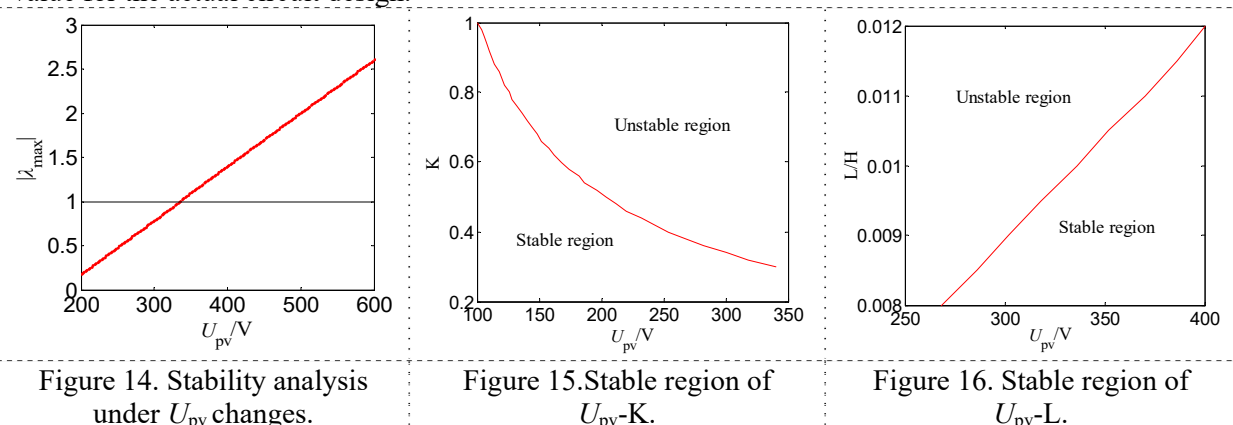
Based on the above discrete model obtained in section 2.2, this section uses the Jacobian matrix method to analyze the stability of system, in order to obtain a stable operating region of system. The Jacobian matrix can be expressed as follows.

$$J = \left( \frac{\partial X_{n+1}}{\partial X_n} + \frac{\partial X_{n+1}}{\partial d_n} \frac{\partial d_n}{\partial X_n} \right) \Bigg|_{\substack{X_n = X_Q \\ d_n = d_Q}} \quad (6)$$

Find maximum eigenvalue  $|\lambda_{\max}|$  of Jacobian matrix for Equation 6, if  $|\lambda_{\max}| < 1$ , system is stability, if  $|\lambda_{\max}| > 1$ , system is unstability,  $|\lambda_{\max}| = 1$ , this circuit parameter value is the boundary point of system between stability and instability [15]. According to discrete model of system shown in (4), the Jacobian matrix of system can be obtained as follows.

$$J = e^{AT} + k\alpha T e^{A(1-d_n)T} (B_2 - B_1) \Bigg|_{X_n = X_Q, d_n = d_Q} \quad (7)$$

The variation curve which is maximum eigenvalue  $|\lambda_{\max}|$  of system Jacobian matrix with the change of bifurcation parameter  $U_{pv}$  can be obtained by the numerical simulation, as shown in figure 14. When  $|\lambda_{\max}| = 1$ , the boundary point of system between stability and instability is  $U_{pv}=339V$ , this is consistent with the conclusion shown in Figure 2. Thus, the stable region of system can be obtained when two parameters change, as shown in Figure 15, 16. This stable region has important reference value for the actual circuit design.



## 5. Conclusion

Photovoltaic inverter system has nonlinear behavior under certain parameters. The bifurcation diagram is used to describe the nonlinear behavior of system when photovoltaic voltage  $U_{pv}$ , filter inductance  $L$ , and proportional coefficient  $K$  are changed, reasonable circuit parameters can make the system run in stable state. According to the actual operating condition of circuit, the nonlinear behavior of system is analysed in detail with  $U_{pv}$  as the bifurcation parameter. Circuit simulation model of system is built in Matlab/Simulink, the correctness of theoretical analysis is verified through time domain waveform and phase-space map, and the influence of bifurcation and chaos on the system spectrum is analyzed through the frequency domain. The experiment shows that nonlinear behavior increases the harmonic content of system and affects the power quality. Finally, the stable region of system operation is given. The research results can guide the correct design of photovoltaic inverter circuit parameters.

## Acknowledgments

This project was supported by National Natural Science Foundation of China (Grant Nos.11262004 and 11562004), Science and Technology Research Project of the Universities in Guangxi (Grant No.

KY2015YB031), and Guilin Scientific Research and Technology Development Plan Project (Grant No. 20170113-4)

### References

- [1] Li S, Liao Z, Luo X, Wei D and Jiang P 2018 *IOP Conf. Ser.: Earth Environ. Sci.* **121** 042007
- [2] Liu H C and Su Z X 2014 *Acta Phys. Sin.* **63** 010505
- [3] Deivasundari P, Uma G and Santhi R 2014 *IET Power Electron.* **7** 340-9
- [4] Wang L, Meng Z, Sun Y and Guo L 2016 *Int. J. Electron.* **104**(1) 157
- [5] Zhusubaliyev Zh T, Mosekilde E, Andriyanov A I and Shein V V 2014 *Physica D: Nonlinear Phenomena* **268** 14-24
- [6] Ming Li, Dong Dai and Xikui Ma 2008 *Circuits Syst Signal Process* **27** 811–831
- [7] Iu H H C and Robert B 2003 *IEEE Trans. Circuits Syst. I Fundam. Theory Appl.* **50** 1125–9
- [8] Wang X M and Zhang B 2009 *Trans. China Electrotech. Soc.* **24**(1) 101
- [9] Wang X M, Zhang B and Qiu D Y 2009 *Acta Phys. Sin.* **58** 2248-54
- [10] Liu H C and Yang S 2013 *Acta Phys. Sin.* **62** 210502
- [11] Wei Jiang, Fang Yuan and Wen-long Hu 2011 *Applied Mechanics and Materials* **39** 1–6
- [12] Bao B C, Zhang X, Xu J P and Wang J P 2013 *IEEE Trans. Electron. Lett.* **49** 287
- [13] A I Andriyanov and D Yu Mikhal'tsov 2016 *IOP Conf. Ser.: Mater. Sci. Eng.* **124** 012041
- [14] Liao Z X, Luo X S and Huang G X 2015 *Acta Phys. Sin.* **64** 1–8
- [15] Yuan X, Cai H and Fu C 2017 *Automation. IEEE.* pp 424–8